April 1997

Preliminary studies of a second generation brachiation robot controller

Jun Nakanishi
Nagoya University

Toshio Fukuda
Nagoya University

Daniel E. Koditschek
University of Pennsylvania, kod@seas.upenn.edu

NOTE: At the time of publication, author Daniel Koditschek was affiliated with the University of Michigan. Currently, he is a faculty member in the Department of Electrical and Systems Engineering at the University of Pennsylvania.

Preliminary studies of a second generation brachiation robot controller

Abstract
We report on our preliminary studies of a new controller for a two-link brachiating robot. Motivated by the pendulum-like motion of an ape's brachiation, we encode this task as the output of a "target dynamical system". Numerical simulations indicate that the resulting controller solves a number of brachiating problems that we term the "ladder", "swing up" and "rope" problems. Preliminary analysis provides some explanation for this success. We discuss a number of formal questions whose answers will be required to gain a full understanding of the strengths and weaknesses of this approach.

NOTE: At the time of publication, author Daniel Koditschek was affiliated with the University of Michigan. Currently, he is a faculty member in the Department of Electrical and Systems Engineering at the University of Pennsylvania.

Proceedings of the 1997 IEEE
International Conference on Robotics and Automation
Albuquerque, New Mexico - April 1997

Preliminary Studies of a Second Generation Brachiation Robot Controller

Jun Nakanishi* and Toshio Fukuda
Dept. of Mechano-Informatics and Systems
Nagoya University
Nagoya, Aichi 464-01, Japan

Daniel E. Koditschek†
Dept. of Electrical Engineering and Computer Science
The University of Michigan
Ann Arbor, MI 48109-2110, USA

Abstract

We report on our preliminary studies of a new controller for a two-link brachiating robot. Motivated by the pendulum-like motion of an ape's brachiation, we encode this task as the output of a "target dynamical system." Numerical simulations indicate that the resulting controller solves a number of brachiating problems that we term the "ladder", "swing up" and "rope" problems. Preliminary analysis provides some explanation for this success. We discuss a number of formal questions whose answers will be required to gain a full understanding of the strengths and weaknesses of this approach.

1 Introduction

This paper presents our preliminary efforts to develop a new controller for a two degree of freedom brachiating robot, following the original success of the second author and colleagues [12, 13]. A brachiating robot dynamically moves from handhold to handhold like an ape swinging its arms. This study considers a simplified two-link point mass lossless model with one actuator at the elbow connecting two arms, each of which has a gripper (see Figure 1). Brachiating robots take an interesting place within the larger category of dynamically dexterous robotics [5] encompassing dexterous manipulation [1, 2, 3, 7, 11], legged locomotion [6, 10, 14, 15] and underactuated mechanisms [16].

Problems of dexterous manipulation have given rise to a growing literature concerned with explicit manipulation of an environment's kinetic as well as potential energy [2, 3, 11, 7, 1]. More specifically, the third author and his students [6, 14, 15] have pursued a number of analytical studies of simple hopping machines that are directly inspired by Raibert's landmark success in legged locomotion [10]. The controller we introduce here bears many similarities to the work of Spong and his students [16], although the more extended problems of slow brachiation require a rather differently conceived notion of target dynamics. Finally, we mention the initial success in robot brachiation achieved by the second author and his student Saito [13, 12].

*The first author was at the Department of Electrical Engineering and Computer Science, the University of Michigan from September, 1995 to August, 1996.

†This work was supported in part by NSF under grant IRI-9510673

1.1 Problem Statement

In our reading of the biomechanics literature [4] we distinguish three variants of brachiation that we will refer to in this paper as the

- Ladder and swing up problem
- Rope problem
- Leap problem

The first arises when an ape transfers from one branch to another and controlling the arm position at next capture represents the central task requirement. A robotics version of this problem has been previously introduced to the literature by the second author and colleagues [12, 13], as mentioned above. The second problem arises from brachiation along a continuum of handholds—a branch or a rope. The third problem arises in the context of fast brachiation where the next branch is far out of reach and the task cannot be accomplished without a large initial velocity and a significant component of free flight. We consider this a fascinating and challenging problem to be addressed when the previous two simpler problems are better understood. Thus, we propose in this paper a control algorithm which is effective for the first two "slow brachiation" problems—i.e. the ladder and swing up and rope problems.

Preuschoft *et al.* [9] studied the mechanics of ape brachiation and identified a close correspondence between slow brachiation and the motion of a simplified pendulum. Accordingly, we have chosen formally to encode the problem of slow brachiation in terms of the output of a target dynamical system—the harmonic oscillator —and this task specification lends a slightly new twist to the traditional view of underactuated mechanisms, as we now discuss.

2 Task Encoding via Target Dynamics

This section presents our control strategy for a two-link brachiating robot. We introduce the notion of "target dynamics" as a particular instance of input/output plant inversion. Specifically, brachiation is encoded as the output of a target dynamical system—a harmonic oscillator, that we must force the robot to mimic.

0-7803-3612-7-4/97 $5.00 ©1997 IEEE

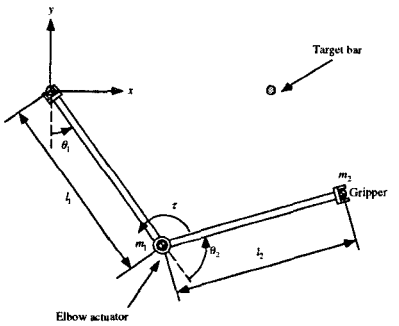

Figure 1: The model of a two-link brachiating robot

2.1 Input/Output Linearization

The notion of target dynamics represents a variant on standard techniques of plant inversion.

Suppose a plant

$$\dot{w} = F(w,v) \quad (1)$$
$$y = H(w) \quad (2)$$

is input/output linearizable. That is, given

$$L_F H(w,v) = DH \cdot F(w,v) \quad (3)$$

if there can be found an implicit function such that for every $u \in \mathcal{U}$ and $w \in \mathcal{W}$, then

$$v = L_F H^{-1}(w,u) \quad (4)$$

implies

$$L_F H(w,v) = u, \quad (5)$$

one calls (4) an input/output linearizing inverse controller in the sense that $\dot{y} = u$.

2.2 Target Dynamics

It is traditional in the underactuated robot control literature to use a linearizing feedback to force an output of a system to track some reference trajectory $r_d(t)$. In the present article, we find it more useful to mimic a reference dynamical system. Consider the dynamics of the two-link brachiating robot which take the form of a standard two-link planer manipulator

$$\dot{Tq} = \mathcal{L}(Tq,\tau) = \begin{bmatrix} \dot{q} \\ M^{-1}\left(-B-k+\begin{bmatrix} 0 \\ \tau \end{bmatrix}\right) \end{bmatrix}. \quad (6)$$

Now identify $w = Tq = [\, q,\ \dot{q}\,]^T$, $\tau = v$ and $\mathcal{L} = F$ in (1).

Suppose we desire the output y to have the characteristics of a target dynamical system

$$\dot{y} = f(y) \quad (7)$$

Then substituting f for u in (4) we have

$$v = L_F H^{-1}(w, f(y)) = L_F H^{-1}(w, f \circ H(w)) \quad (8)$$

According to the biomechanics literature [9] slow brachiation of apes resembles the motion of a pendulum. Although the ape's moment of inertia varies during the swing according its change of posture, the motion of a simplified pendulum gives a fairly good approximation. Motivated by this pendulum-like motion of brachiation, we choose to encode the task in terms of the even simpler linearized version,

$$y = Tx = \begin{bmatrix} x \\ \dot{x} \end{bmatrix},\ f_\omega(Tx) = \begin{bmatrix} 0 & 1 \\ -\omega^2 & 0 \end{bmatrix} Tx, \quad (9)$$

that will serve as the target dynamical system in this paper.

Thus, we will find it useful to introduce a submersion arising from the change of coordinates from joint space to polar coordinates on $\mathbb{R}^2$,

$$\begin{bmatrix} r \\ \theta \end{bmatrix} = \tilde{q} = \bar{g}(q) = \begin{bmatrix} l\sqrt{2(1+\cos\theta_2)} \\ \theta_1 + \frac{1}{2}\theta_2 \end{bmatrix}. \quad (10)$$

Specifically, we will take the second component of (10).

$$x = h(q) := \theta = [0,1]\,\bar{g}(q) = \theta_1 + \frac{1}{2}\theta_2 \quad (11)$$

so that the application of (8) in the example of interest takes the form

$$\begin{aligned} \tau &= \tau_\omega := L_F H^{-1}(Tq, f_\omega \circ Th(Tq)) \\ &= \left(D_q h \begin{bmatrix} n_{12} \\ n_{22} \end{bmatrix}\right)^{-1} \left[-\omega^2\theta - (\dot{D_q h})\dot{q} + D_q h M^{-1}(B+k)\right] \\ &= \frac{1}{n_{12}+\frac{1}{2}n_{22}} \left[-\omega^2(\theta_1+\frac{1}{2}\theta_2) + (n_{11}+\frac{1}{2}n_{21})(B_1+k_1)\right] \\ &\quad + B_2 + k_2 \end{aligned} \quad (12)$$

where

$$M^{-1} = \begin{bmatrix} n_{11} & n_{12} \\ n_{21} & n_{22} \end{bmatrix}$$

Notice that

$$D_q h \begin{bmatrix} n_{12} \\ n_{22} \end{bmatrix} = n_{12} + \frac{1}{2}n_{22} = \frac{m_1 l^2}{2\det(M)} \neq 0 \quad (13)$$

i.e., the invertibility condition of $L_F H$ is satisfied in the particular setting of concern.

3 Ladder and Swing up Problem

We now move on to the specific problems of robot brachiation. First, we apply the target dynamics method to the ladder problem. Then, we consider the swing up problem. The target dynamics is modified to introduce a limit cycle to achieve the task. Numerical simulations are provided to suggest the effectiveness of the proposed algorithms.

3.1 Ladder problem

As we have pointed out, the ladder problem arises when an ape transfers from one branch to another and the

control of arm position at the next capture represents the control task requirement. Here, we restrict our attention to brachiation on a set of evenly spaced bars at the same height. The target dynamics method is applied to the ladder problem. We show how a symmetry property of an appropriately chosen target system— (9) in the present case—can solve this problem.

3.1.1 Neutral Orbits, $\mathcal{N}$

This section follows closely the ideas originally developed in [14, 15]. We discuss a reverse time symmetry inherent in the brachiating robot's dynamics. First, we show that the natural dynamics of the two-link brachiating robot admit a reverse time symmetry, S. Then, we give a condition under which feedback laws result in closed loops that still admit S. Lastly, following Raibert [10], we introduce the notion of the neutral orbits of the symmetry, and show how they may be used to solve the ladder problem. In the sequel, we will denote the integral curve of a vector field f by the notation f^t.

Definition 3.1 *$f : \mathcal{X} \to T\mathcal{X}$ admits a reverse time symmetry $S : \mathcal{X} \to \mathcal{X}$ if and only if $S \circ f^t = f^{-t} \circ S$.*

Note that when S is linear, this definition might by equivalently stated as $S \circ f = -f \circ S$. In this paper, we are concerned specifically with the symmetry operator

$$S = \begin{bmatrix} -I_2 & 0 \\ 0 & I_2 \end{bmatrix}. \tag{14}$$

(where I_2 denotes the 2×2 identity matrix).

Now, supposing we have chosen a feedback law, $\tau(q, \dot{q})$, denote the closed loop dynamics of the robot as

$$\dot{Tq} = \mathcal{L}_\tau(Tq) = \mathcal{L}\left(Tq, \tau(Tq)\right) \tag{15}$$

Say that τ "respects S" if and only if $\mathcal{L}_\tau$ admits S.

Proposition 3.2 *The closed loop dynamics $\mathcal{L}_\tau$ admits S, i.e., $S \circ \mathcal{L}_\tau(Tq) = -\mathcal{L}_\tau \circ S(Tq)$ if and only if $\tau(q, \dot{q})$ has the property $\tau(-q, \dot{q}) = -\tau(q, \dot{q})$.*

This result follows from direct computation, and we refer the reader to [8] for the details.

Define the fixed points of the symmetry S to be

$$\mathrm{Fix}S := \{Tq \in TQ \mid S(Tq) = Tq\} \tag{16}$$

In the present case, i.e., for S in (14) note that

$$\mathrm{Fix}S = \{(q, \dot{q}) \in TQ | q = 0\}$$

Define the set of "neutral orbits" to be the integral curves which go through the fixed point set,

$$\mathcal{N} := \bigcup_{t \in \mathbb{R}} \mathcal{L}^t(\mathrm{Fix}S) \tag{17}$$

Note that a neutral orbit has a symmetry property about its fixed point—namely, if $Tq_0 \in \mathrm{Fix}S$, then

$$S \circ \mathcal{L}^t(Tq_0) = \mathcal{L}^{-t} \circ S(Tq_0) = \mathcal{L}^{-t}(Tq_0)$$

3.1.2 The Ceiling, $\mathcal{C}$, and its Neutral Orbits

Define the "ceiling" to be those configurations where the hand of the robot reaches the height $y = 0$ as depicted in Figure 2.

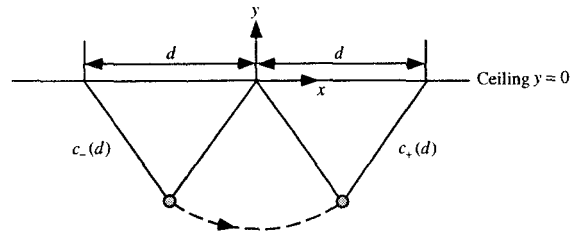

Figure 2: A ceiling configuration. The ceiling is parametrized by the distance between the grippers d. A left branch $c_-(d)$ and right branch $c_+(d)$ are defined in this manner.

$$\mathcal{C} = \{q \in Q | \cos\theta_1 + \cos(\theta_1 + \theta_2) = 0\}. \tag{18}$$

Note that $\mathcal{C}$ can be parameterized by two branches,

$$\mathcal{C} = \mathrm{Im}\, c_- \cup \mathrm{Im}\, c_+ \tag{19}$$

of the maps

$$c_\pm(d) = \begin{bmatrix} \pm \arcsin\left(\frac{d}{2l}\right) \\ \pm\left[\pi - 2\arcsin\left(\frac{d}{2l}\right)\right] \end{bmatrix}. \tag{20}$$

In the sequel, we will be particularly interested in initial conditions of (15) originating in the zero velocity sections of the ceiling that we denote $T\mathcal{C}_0$. Now note that $S(T\mathcal{C}_0) \subseteq T\mathcal{C}_0$ since

$$S\begin{bmatrix} c_-(d) \\ 0 \\ 0 \end{bmatrix} = \begin{bmatrix} c_+(d) \\ 0 \\ 0 \end{bmatrix}. \tag{21}$$

Proposition 3.3 *If a feedback law, τ, respects S and if $\begin{bmatrix} c_-(d) \\ 0 \\ 0 \end{bmatrix} \in \mathcal{N} \cap T\mathcal{C}_0$, then there can be found a time $t_N \in \mathbb{R}$ such that if $\nu = \frac{t_N}{4}$ then*

$$\mathcal{L}_\tau^{2\nu}\left(\begin{bmatrix} c_-(d) \\ 0 \\ 0 \end{bmatrix}\right) = \begin{bmatrix} c_+(d) \\ 0 \\ 0 \end{bmatrix} \tag{22}$$

i.e., a time at which the left branch at zero velocity in the ceiling reaches the right branch in the ceiling also at zero velocity.

Again we refer the reader to [8] for details of the proof of Proposition 3.3. Thus, we conclude that any feedback law, τ, which respects S, solves the ladder problem, assuming we can find a d such that $[\, c_-(d),\ 0\,]^T \in \mathcal{N}$.

Note that finding such a ceiling point requires solving the equation

$$\Phi(d, t_N) = [\ I_2\ ,\ \ 0\ ]\mathcal{L}_\tau^\nu \left(\begin{bmatrix} c_-(d) \\ 0 \\ 0 \end{bmatrix} \right) = \begin{bmatrix} 0 \\ 0 \end{bmatrix} \quad (23)$$

, where $\nu = \frac{t_N}{4}$, for d and t_N simultaneously. Of course solving this equation is very difficult: it requires a "root finding" procedure that entails integrating the dynamics, $\mathcal{L}$.

3.1.3 Application of Target Dynamics

Now we apply the notion of target dynamics described in (9). The feedback law to achieve this is given by (12). Notice that τ_ω respects S since $\tau_\omega(-q, \dot{q}) = -\tau_\omega(q, \dot{q})$. Notice, as well, that (9) has a very nice property relative to the difficult root finding problem (23). Namely, using this control algorithm, t_N is given by

$$t_N(\tau_\omega) = \frac{2\pi}{\omega} \quad (24)$$

because θ follows the target dynamics $\ddot{\theta} = -\omega^2\theta$. In this light, then, we need merely solve (23) for d. More fomally, we seek an implicit function $d^* = \lambda^{-1}(\omega)$ such that $\Phi\left(\lambda^{-1}(\omega), \frac{2\pi}{\omega}\right) = 0$. Of course, we are more likely in practice to take an interest in tuning ω as a function of a desired d^*. Thus, we are most interested in determining

$$\omega = \lambda(d^*). \quad (25)$$

In general, we can expect no closed form expression for λ or λ^{-1}, and we resort instead to a numerical procedure for determining an estimate, $\hat{\lambda}$. The details of the numerical procedure is discussed in [8]. We plot in Figure 3 a particular instance of $\hat{\lambda}$ for the case where the robot parameters are $l = 1, m_1 = 3, m_2 = 1$. We will use these parameter values throughout the sequel for the sake of comparison between this and subsequent figures.

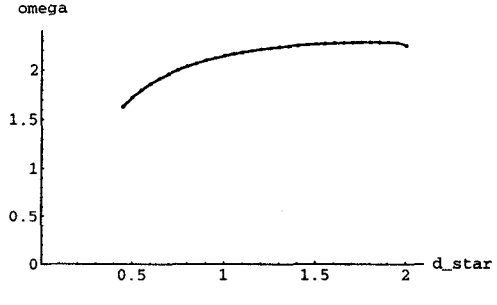

Figure 3: Numerical approximation $\omega = \hat{\lambda}(d^*)$. Target dynamics controller, τ_ω, is tuned according to this mapping, $\hat{\lambda}$, that is designed to locate neutral orbits originating in the ceiling.

3.1.4 Simulation

Consider the case $d^* = 1.4$ for this parameter set above. The initial condition of the robot is $Tq_0 = [\ c_-(d^*),\ 0\ ]^T$. From the numerical solution depicted in Figure 3, $\omega = \hat{\lambda}(1.4) = 2.2512$. Figure 4 shows the resulting movement of the robot. The closed loop dynamics have a neutral orbit which achieves the task.

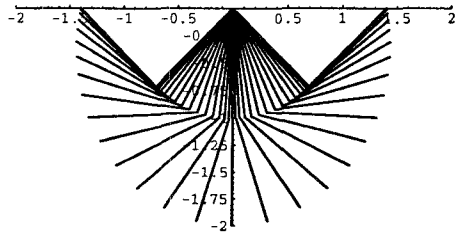

Figure 4: Movement of the robot. The symmetry properties of the neutral orbit from the ceiling solves the ladder problem.

3.2 Swing up Problem

The swing up problem entails swinging up from the suspended posture at rest and catching the next bar. In order to achieve this task it is necessary not only to pump up the energy in a suitable fashion but also to control the arm position at the capture of the next target bar. This suggests that we need to introduce a stable limit cycle to the system with suitable magnitude and relative phase in state. The idea we present here is a simple modification of the foregoing target dynamics. We define the "pseudo energy" with respect to the target variable and add a compensation term to the target dynamics in order to introduce the desired limit cycle.

3.2.1 Modified Target Dynamics

As we have mentioned, swing up requires energy pumping in a suitable fashion. To achieve this we modify the target dynamics (9) as

$$\dot{Tx} = \begin{bmatrix} 0 & 1 \\ -\omega^2 & -K_e(\bar{E} - \bar{E}^*) \end{bmatrix} Tx := f_{\bar{E}^*}(Tx) \quad (26)$$

where, $x = \theta = \theta_1 + \frac{1}{2}\theta_2$ as defined in (11)
K_e: a positive constant
$\bar{E} := \frac{1}{2}\dot{\theta}^2 + \frac{1}{2}{\omega_T}^2\theta^2$: "pseudo energy"
$\bar{E}^*$: the desired pseudo energy level

To achieve this target dynamics, the control law is formulated as

$$\begin{aligned} \tau_{\bar{E}^*} &= L_F H^{-1}(Tq, f_{\bar{E}^*} \circ Th(Tq)) \\ &= \left(D_q h \begin{bmatrix} n_{12} \\ n_{22} \end{bmatrix}\right)^{-1} \left[-\omega^2\theta - K_e(\bar{E} - \bar{E}^*)\dot{\theta} \right. \\ &\quad \left. - (\dot{D_q h})\dot{q} + D_q h M^{-1}(V + k)\right] \\ &= \frac{1}{n_{12} + \frac{1}{2}n_{22}} \left[-\omega^2(\theta_1 + \frac{1}{2}\theta_2) - K_e(\bar{E} - \bar{E}^*)(\dot{\theta_1} + \frac{1}{2}\dot{\theta_2}) \right. \\ &\quad \left. + (n_{11} + \frac{1}{2}n_{21})(B_1 + k_1)\right] + B_2 + k_2 \end{aligned} \quad (27)$$

Now consider the time derivative of $\bar{E}$ along the motion

$$\dot{\bar{E}} = -K_e(\bar{E} - \bar{E}^*)\dot{\theta}^2 \tag{28}$$

If $\bar{E} > \bar{E}^*$ then the pseudo energy $\bar{E}$ decreases, and if $\bar{E} < \bar{E}^*$ then $\bar{E}$ increases. Therefore, $\bar{E}$ will converge to the desired level $\bar{E}^*$ eventually. This implies that the target dynamics with respect to θ coordinates has a stable limit cycle whose trajectory is characterized by $\frac{1}{2}\dot{\theta}^2 + \frac{1}{2}\omega^2\theta^2 = \bar{E}^*$ on the phase plane of $(\theta, \dot{\theta})$.

Although we have experienced very favorable results in numerical simulations introducing the desired limit cycle to the "target variable" using the ideas set out above, the procedure remains somewhat ad hoc. Most importantly, we need to bring the effective actuated portion of the state space, θ, to the right pseudo energy level, while simultaneously ensuring that the unactuated degree of freedom, r, coincide with the regulated length, d^*, when the trajectory enters the ceiling, $\mathcal{TC}$.

As the simulation suggests, some experience is helpful in determining the proper choice of the parameters K_e, ω to give the desired motion of the robot to achieve the task. For example, large K_e seems to yield chaotic motion and small choice of K_e is preferred. Of course, an elucidation of these relationship awaits a proper mathematical analysis.

3.2.2 Simulation

Suppose the next target bar is located at the distance $d^* = 1.4$. The initial condition is $q_0 = [\ 0.01,\ 0\ ]^T$ and $\dot{q}_0 = 0$. We choose the parameters in the target dynamics as $\omega = \hat{\lambda}(1.4) = 2.2512$, $K_e = 0.75$, $\bar{E}^* = \frac{1}{2}\omega^2\left(\frac{\pi}{2}\right)^2$.

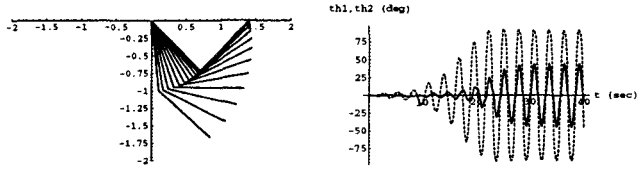

Figure 5: Left: The movement at the capture of a bar $t = 33 \sim 33.625$ sec. The swing up task is achieved under the modified target dynamics. Right: Joint trajectories (θ_1: solid, θ_2: dashed). The desired limit cycle is achieved.

Figure 5 depicts the movement of the robot at the capture of a bar, and the joint trajectories of θ_1, θ_2. These simulation results suggest that the robot can achieve the swing up and catching task via the modified target dynamics.

4 Rope problem

In this section, we consider the rope problem: brachiation along a continuum of handholds such as afforded by a branch or a rope. First, the average horizontal velocity is characterized as a result of the application of the target dynamics controller, τ_ω, introduced above. Then, we consider the regulation of horizontal velocity using this controller. An associated numerical "swing map" suggests that we indeed can achieve good local regulation of the foward velocity through the target dynamics method.

4.1 The Iterated Ladder Trajectory Induces a Horizontal Velocity

Supposing that the robot starts in the ceiling with zero velocity, then it must end in the ceiling under the target dynamics controller since θ follows the dynamics $\ddot{\theta} = -\omega^2\theta$. However, if d and ω are not "matched" as $\omega = \lambda(d)$, then the trajectory ends in the ceiling, $Tq \in \mathcal{TC}_+$, with $\dot{\theta} = 0$ but $r \neq d$ and $\dot{r} \neq 0$. We have found from our numerical studies [8] that when $d = d^* + \delta$ for small δ, then $\dot{r}$ at $Tq \in \mathcal{TC}_+$ is also small. Assuming that any such small nonzero velocity is killed in the ceiling, brachiation may be iterated by opening and closing the grippers at left and right ends. Imagine that the robot starts the swing and by grasping the bar with its gripper firmly in the ceiling damps out the kinetic energy before opening the other gripper and beginning the next swing. We will call such a maneuver the Iterated Ladder Trajectory ("ILT").

It is natural to inquire as to how quickly horizontal progress can be made along the ladder in so doing. When a gripper moves a distance $2d^*$ in the course of the ladder trajectory, and if the trajectory is immediately repeated, as described above, then the body, m_1, will also move a distance of d^* each swing, hence, its average horizontal velocity will be

$$\bar{\dot{h}} = \frac{d^*\omega}{\pi} = \frac{d^*\lambda(d^*)}{\pi} := \tilde{V}_2(d^*) \tag{29}$$

according to the discussion in Section 3.1. In Figure 6, we now plot the ceiling-to-velocity map $\bar{\dot{h}} = \tilde{V}_2(d^*)$ for the robot parameters $l = 1, m_1 = 3, m_2 = 1$, where $\tilde{V}_2$ is computed using the numerical approximation, $\hat{\lambda}$ discussed in Section 3.1.3.

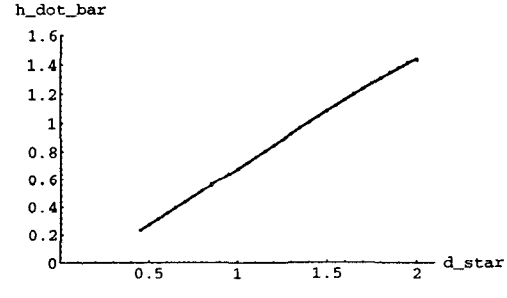

Figure 6: The ceiling-to-velocity map, $\tilde{V}_2$. This mapping is inverted to obtain the desired forward velocity $\bar{\dot{h}}^*$.

4.2 Inverting the Ceiling-to-Velocity Map

Consider now the task of obtaining the desired forward velocity $\bar{\dot{h}}^*$ of brachiation. If $\tilde{V}_2$ is invertible, then $d^* = \tilde{V}_2^{-1}(\bar{\dot{h}}^*)$ and we can tune ω in the target dynamics as

$$\omega = \lambda \circ \tilde{V}_2^{-1}(\bar{\dot{h}}^*) \tag{30}$$

to achieve a desired $\bar{\dot{h}}^*$ where λ is again the mapping (25). We have found in our numerical work that $\tilde{V}_2$ does, indeed, seem to be nicely invertible as suggested by the particular case of Figure 6.

4.3 Horizontal Velocity Regulation

Consider the ceiling condition with zero velocity

$$T\mathcal{C}_{0\pm} = \left\{ \begin{bmatrix} c_\pm(d) \\ 0 \\ 0 \end{bmatrix} \in T\mathcal{C} \mid d \in [0, 2l] \right\} \tag{31}$$

Define the maps, $C_\pm$, and their inverses, $C_\pm^{-1}$, as

$$C_\pm : [0, 2l] \rightarrow T\mathcal{C}_{0\pm} : d \mapsto \begin{bmatrix} c_\pm(d) \\ 0 \\ 0 \end{bmatrix} \tag{32}$$

$$C_\pm^{-1} : T\mathcal{C}_{0\pm} \rightarrow [0, 2l] : \begin{bmatrix} c_\pm(d) \\ 0 \\ 0 \end{bmatrix} \mapsto d \tag{33}$$

A target dynamics controller (9) gives

$$\mathcal{L}_{\tau_\omega}^{2\nu} \circ C_-(d) \in T\mathcal{C}_+ \text{ , where } \nu = \frac{\pi}{2\omega} \tag{34}$$

since θ follows the dynamics $\ddot{\theta} = -\omega^2\theta$. Now, if $\omega = \lambda(d)$, then

$$\mathcal{L}_{\tau_\omega}^{2\nu} \circ C_-(d) = C_+(d) = \begin{bmatrix} c_+(d) \\ 0 \\ 0 \end{bmatrix} \in T\mathcal{C}_{0+} \tag{35}$$

, where $\nu = \frac{\pi}{2\omega}$, because of the symmetry properties of the neutral orbits, demonstrated in Proposition 3.3.

Define a projection Π, from the ceiling's tangents into the zero velocity section,

$$\Pi : T\mathcal{C}_\pm \mapsto T\mathcal{C}_{0\pm}. \tag{36}$$

In other words, Π is a map that "kills" any velocity in the ceiling. We introduce this projection to model the ILT maneuver in cases when $\dot{r} \neq 0$ for $Tq \in T\mathcal{C}$.

We now have from (34)

$$\Pi \circ \mathcal{L}_{\tau_\omega}^{2\nu} \circ C_-(d) \in T\mathcal{C}_{0+} \text{ , where } \nu = \frac{\pi}{2\omega} \tag{37}$$

hence we may define a "swing map", σ_ω, as a transformation of $[0, 2l]$ into itself,

$$\sigma_\omega(d) := C_+^{-1} \circ \Pi \circ \mathcal{L}_{\tau_\omega}^{2\nu} \circ C_-(d) : [0, 2l] \rightarrow [0, 2l] \tag{38}$$

Note that if $\omega = \omega^* = \lambda(d^*)$, then

$$\sigma_\omega(d^*) = d^* \tag{39}$$

that is, d^* is a fixed point of the appropriately tuned swing map.

It is now clear that the dynamics of the ILT maneuver can be modeled by the iterates of this swing map, σ_ω. Namely, suppose we iterate by setting the next initial condition in the ceiling to be,

$$Tq_0[k+1] = C_-(\sigma_\omega(d[k])) \tag{40}$$

Numerical evidence suggests that the iterated dynamics converges, $\lim_{k\rightarrow\infty} \sigma_{\omega^*}^k(d) = d^*$, when d is in the neighborhood of d^* as depicted in Figure 7 (local asymptotic stability of the fixed point d^*). We plot the swing map calculated numerically for the case where $\bar{h} = 0.9, d^* = 1.26815, \omega = 2.2270$ and the robot parameters are $l = 1, m_1 = 3, m_2 = 1$ (see Figure 7).

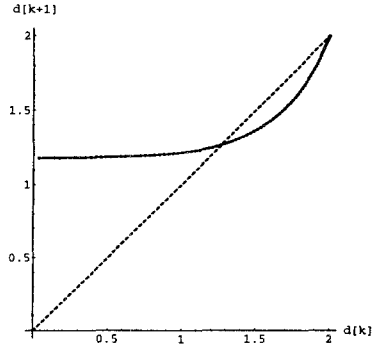

Figure 7: Swing map, σ_ω, (solid) and identity (dashed) for the case $\bar{h} = 0.9, d^* = 1.26815, \omega = 2.2270$ where $\hat{\omega}^* = \lambda(d^*)$, and the robot parameters are $l = 1, m_1 = 3, m_2 = 1$. This swing map has an attracting fixed point at d^*.

4.4 Simulation

Suppose we want to achieve the desired horizontal velocity, $\bar{\dot{h}}^* = 0.9$(m/s). The parameters of the robot are $l = 1, m_1 = 3, m_2 = 1$. The procedure to obtain the numerical approximation of (30) as follows:

First, the ceiling-to-velocity map (29) is approximated by the third order polynominal.

$$\bar{\dot{h}} = -0.0446d^{*3} + 0.1278d^{*2} + 0.7052d^* - 0.1040 \tag{41}$$

Then, to obtain the approximating solution to $\tilde{V}_2^{-1}(0.9)$, (41) is solved for d^* numerically by setting $\bar{\dot{h}} = 0.9$, and we get $d^* = 1.26815$. Lastly, from the numerical solution depicted in Figure 3, $\omega = \hat{\lambda}(1.2682) = 2.2270$.

First, consider ILT with the proper initial condition

$$Tq_0^* = \begin{bmatrix} c_-(d*) \\ 0 \end{bmatrix} \tag{42}$$

which is proper in the sense $\bar{h}^* = \tilde{V}_2(d^*)$. The simulation result in this case is shown in Figure 8—a faithfully executed ILT at d^*.

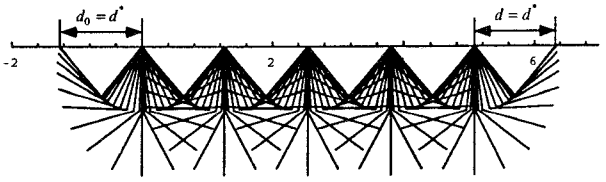

Figure 8: Brachiation along the bar with the initial condition (42). The desired locomotion with the fixed point d^* is achieved.

Suppose, instead, that assuming $\omega = \lambda(d^*)$ but the initial d_0 is wrong. We present simulation results with the initial condition

$$Tq_0 = \begin{bmatrix} c_-(d^* + \delta) \\ 0 \end{bmatrix}, \text{where } \delta = -0.3 \qquad (43)$$

in Figure 9. As the numerical swing map of (7) suggets, we can nevertheless achieve the desired locomotion, i.e., $d \to d^*$.

With the assumption that any velocity in the ceiling is killed, the size of the domain of attraction to d^* under σ_{ω^*} is fairly large according to the numerical evidence shown in Figure 7.

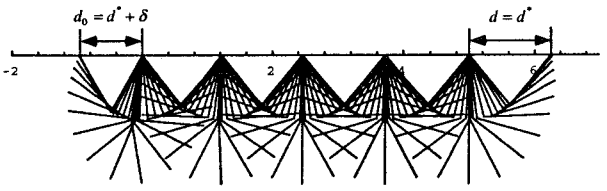

Figure 9: Brachiation along the bar with the initial condition (43). Convergence of $d \to d^*$ is illustrated as the numerical swing map (Figure 7) indicates.

5 Conclusion

We have presented some preliminary studies of a new brachiating controller for a simplified two-link robot. The algorithm uses a target dynamics method to solve the ladder, swing up and rope problems. These tasks are encoded as the output of a target dynamical system inspired by the pendulum-like motion of an ape's (slow) brachiation. We provide numerical simulations suggesting the effectiveness of the proposed algorithm. However, these numerical results also indicate that the sensitivity of the linearization scheme (12) to the required kinematic and dynamical parameters, l, m_1 and m_2, may damage the resulting closed loop motion when available estimates are not extremely close to the true values. In general, even with exact calibration data, our observations suggest that the approach taken in this paper works well only when roughly $\omega \propto \frac{1}{\sqrt{l}}$ and m_1 is larger than m_2. Under these circumstances, we present more numerical evidence in [8] that the proposed algorithm is practically feasible in terms of the required actuator torque and power.

References

[1] Andersson, R. L. *A Robot Ping-Pong Player: Experiment in Real-Time Intellgent Control.* MIT Press, 1988.

[2] Bühler, M., Koditschek, D. E., and Kindlmann, P. J. A family of robot control strategies for intermittent dynamical environments. *IEEE Control Systems Magazine*, pages 16–22, February 1990.

[3] Burridge, R. R., Rizzi, A. A., and Koditschek, D. E. Toward a systems theory for the composition of dynamically dexterous behaviors. In *7th Internatinal Symposium on Robotics Research*, 1995.

[4] Eimerl, S. and DeVore, I. *The Primates.* TIME-LIFE BOOKS, 1966.

[5] Koditschek, D. E. Dynamically dexterous robots. In Spong, M. W., Lewis, F. L., and Abdallah, C. T., editors, *Robot Control: Dynamics, Motion Planning and Analysis*, pages 487–490. IEEE Press.

[6] Koditschek, D. E. and Bühler, M. Analysis of a simplified hopping robot. *International Journal of Robotics Research*, 10(6):587–605, December 1991.

[7] Lynch, K. M. *Nonprehensile Robotic Manipulation: Controllability and Planning.* PhD thesis, Carnegie Mellon University, The Robotics Institute, March 1996.

[8] Nakanishi, J., Fukuda, T., and Koditschek, D. E. Preliminary analytical approach to a brachiation robot controller. Technical report: CGR 96-08 / CSE TR 305-96, The Univ. of Michigan, EECS Depertment, August 1996.

[9] Preuschoft, H. and Demes, B. Biomechanics of brachiation. In Preuschoft, H., Chivers, D. J., Brockelman, W. Y., and Creel, N., editors, *The Lesser Apes*, pages 96–228. Edinburgh University Press, 1984.

[10] Raibert, M. H. *Legged Robots that Balance.* MIT Press, 1986.

[11] Rizzi, A. A., Whitcomb, L. L., and Koditschek, D. E. Distributed real-time control of a spatial robot juggler. *IEEE Computer*, pages 12–24, May 1992.

[12] Saito, F. *Motion Control of the Brachiation Type of Mobile Robot.* PhD thesis, Nagoya University, March 1995. (in Japanese).

[13] Saito, F., Fukuda, T., and Arai, F. Swing and locomotion control for a two-link brachiation robot. *IEEE Control Systems Magazine*, 12:5–12, February 1994.

[14] Schwind, W. J. and Koditschek, D. E. Control the forward velocity of the simplified planner hopping robot. In *IEEE International Conference on Robotics and Automation*, 1995.

[15] Schwind, W. J. and Koditschek, D. E. Characterization of monopod equilibrium gaits. In *IEEE International Conference on Robotics and Automation*, 1997. (accepted).

[16] Spong, M. The swing up control problem for the acrobot. *IEEE Control Systems Magazine*, 15:49–55, February 1995.